Available online at www.sciencedirect.com
SCIENCE DIRECT®
Journal of Nuclear Materials 348 (2006) 1–17
journal of nuclear materials
www.elsevier.com/locate/jnucmat

Addition versus radiolytic production effects of hydrogen peroxide on aqueous corrosion of UO_2

C. Corbel [a,*], G. Sattonnay [a,b], S. Guilbert [c], F. Garrido [b], M.-F. Barthe [c], C. Jegou [d]

[a] *Commissariat à l'Energie Atomique, CEA-Saclay, DSM/DRECAM/SCM Laboratoire CEA de radiolyse, Bât. 546, F-91191 Gif sur Yvette cedex, France*
[b] *Centre de Spectrométrie Nucléaire et de Spectrométrie de Masse, IN2P3, Université Paris Sud, Bât. 104-108, F-91405 Orsay cedex, France*
[c] *CNRS-Centre d'Etudes et de Recherches par Irradiation, 3A rue de la Férollerie, F-45071 Orléans cedex 2, France*
[d] *Commissariat à l'Energie Atomique, CEA-Marcoule, Rhône Valley Research Center, DTCD/SECM/LMPA, BP 17171, 30207 Bagnols-sur-Cèze cedex, France*

Received 6 September 2004; accepted 10 May 2005

Abstract

The effects of hydrogen peroxide, H_2O_2, on UO_2 corrosion is investigated in aerated deionized water in two types of situations. The H_2O_2 species is either added to water or produced by radiolysis at UO_2/H_2O interfaces. The concentrations vary in the range 10^{-5}–10^{-1} mol l^{-1}. The radiolysis is induced by irradiating the UO_2/H_2O interfaces with a He^{2+}-beam emerging from the UO_2 discs into the solutions. Both the evolution of the aqueous solutions and the UO_2 surfaces are characterised. In both types of experiments, the alteration of UO_2 results in the formation of the same secondary phase, an hydrated uranium peroxide called studtite ($UO_2(O)_2 \cdot 4H_2O$). However, the uranium release at the interface differs strikingly. It is much higher when H_2O_2 is produced by irradiation than when it is simply added. Furthermore, it varies in opposite direction as a function of the H_2O_2 concentration. This gives evidence that the chemistry at the UO_2 interface under irradiation differs significantly from the chemistry induced by simply adding H_2O_2 to the solution. Rutherford backscattering spectrometry is used to determine the growth rate of the corrosion layer. For H_2O_2 addition, the layer thickness increases with increasing leaching time, although as time increases, the U release tends towards zero. It is possible to establish the first empirical equation relating the corrosion rates to the added H_2O_2 concentrations. For H_2O_2 radiolytic production, the growth is continuous as irradiation time increases but the growth rate seems to decrease as the layer grows and to reach a limit.

PACS: 82.65.−i; 82.50.Gw; 81.05.Je; 81.65.−b

* Corresponding author. Address: LSI Ecole Polytechnique, Palaiseau, France. Tel.: +33 1 01 69 33 46 98 21; fax: +33 1 01 69 33 30 22.
E-mail address: ccorbel@cea.fr (C. Corbel).

0022-3115/$ - see front matter © 2005 Elsevier B.V. All rights reserved.
doi:10.1016/j.jnucmat.2005.05.009

1. Introduction

The uranium dioxide fuels used in commercial nuclear reactors are by far the most significant to repository performance. The fission reactions that occur in these fuels during their use in reactors modify their chemical composition, activity and microstructure. Spent uranium dioxide nuclear fuels, UOX, are gamma, beta and alpha radioactive materials with an activity depending on their burn-up and storing age. Any environmental assessment of spent nuclear fuel disposal requires a prediction of the release of uranium from the fuel once contact with groundwater is established. One important process that may affect spent fuel dissolution is the production of radiolytic species in the surrounding water submitted to its radiation. This production modifies the redox conditions and, according to some authors, can cause oxidising conditions near the spent nuclear fuel surface even in disposal vaults where groundwater is reducing [1]. The oxidation state of UOX surface is expected to affect strongly UOX dissolution in analogy to UO_2 that is reported to significantly release uranium once the surface reaches the composition $UO_{2.33}$ [1–3]. Radiolysis is consequently one process that needs to be considered in spent fuel evolution in presence of water [4–6]. The difficulty is that there is little knowledge on the basic mechanisms that occur at UOX/H_2O interfaces. Model experiments need to be conducted [7,8].

The radiolysis of water produces both molecular (H_2O_2, H_2) and radical ($^{\bullet}OH$, $O_2^{\bullet-}$, $HO_2^{\bullet}$, e_{aq}^-, $H^{\bullet}$) products, the concentrations of which depend on both the nature of the ionizing radiation and the radiation dose deposited in water [9,10]. Model experiments related to UOX/H_2O interfaces can be conducted on UO_2/H_2O interfaces irradiated by external gamma sources or electron or He^{2+} ion beams. Recently, such an approach has been proposed to investigate how $^4He^{2+}$ ion (alpha) emission from UO_2 surfaces may affect both the release of uranium at UO_2/water interfaces and the alteration of UO_2 surfaces [11–13]. A high-energy beam of $^4He^{2+}$ ions supplied by a cyclotron irradiates an UO_2/H_2O interface and passes through the UO_2 disc and emerges into the deionized water in contact with the disc. This work demonstrates that $^4He^{2+}$ ion irradiation of UO_2/H_2O interfaces at high fluxes, of the order of 10^{10}–10^{11} He^{2+} cm^{-2} s^1, leads to a strong alteration of the UO_2 surface in aerated deionized water. Irradiation enhances the U release in the solutions and induces the formation of a secondary phase of hydrated uranium peroxide on the UO_2 surface. The authors [11–13] propose that the formation of this alteration product is related to the production of the radiolytic species H_2O_2 in water.

The investigation of UO_2 dissolution in deionized water where various concentrations of H_2O_2 are added can give useful information for an evaluation of the radiolysis effect due to H_2O_2. Nevertheless, few works [14–22] on the H_2O_2 effects on UO_2 corrosion have been carried out. The present work aims to compare the effects of H_2O_2 addition and radiolytic production on the evolution of UO_2/H_2O interfaces. Two kinds of experiments are carried out. The first one is a kinetic study of the UO_2 corrosion as a function of H_2O_2 concentration when H_2O_2 is added in aerated deionized water. The second one deals with the corrosion kinetic of UO_2 when H_2O_2 is radiolytically produced in aerated deionized water at the UO_2/H_2O interface water under He^{2+} ion beam. The same leaching cells being used in both types of experiments, the solid/water geometry at the interface and the ratio of the UO_2 surface to water volume are the same for the leachings in presence of added or radiolytically produced H_2O_2.

2. Experimental procedure

2.1. Materials

The UO_2 material used here is isotopically depleted and contains 0.2 at.% ^{235}U. The 30 UO_2 discs mounted on the leaching cells are cut from sintered UO_2 pellets with a density, $\rho v = 10.45\ g\ cm^{-3}$, close to the UO_2 density, $10.98\ g\ cm^{-3}$. The 8.2 mm diameter discs are thin with thickness $275 \pm 5\ \mu m$. One face of the discs is mechanically mirror-like polished. At the end of the polishing, the discs are annealed under a mixture of H_2/Ar (8%) gas at 1400 °C to remove polishing damage and adjust the oxygen to metal ratio to the stoichiometric value (O/U ≅ 2.0).

2.2. Leaching experiments

The leaching experiments with H_2O_2 either added or radiolytically produced use the same type of Teflon leaching cell and are carried out at room temperature. Each UO_2 disc is mounted in the leaching cell so that, when the cell is filled, the polished face of the disc has a centered surface, $S = 0.283\ cm^2$ (6 mm diameter) leached by a volume, $V = 10$ ml, of solution. The ratio of the leached surface to the solution volume has then the low value $S/V = 0.0283\ cm^{-1}$ ($2.8\ m^{-1}$). No correction is applied to the specific surface area that is taken equal to $ss\ (cm^{-2}\ g^{-1}) = (M_{mol}(UO_2))^{-1} \times (M_{mol}(UO_2)/\rho v)^{2/3}$, i.e. $3.2 \times 10^{-6}\ m^2\ g^{-1}$. The aerated deionized water used to prepare the solutions where H_2O_2 is either added or radiolytic produced has a 18 MΩ cm resistivity and a pH of about 6. For H_2O_2 addition, the cell is filled with aerated deionized water containing H_2O_2 concentrations in the range 5×10^{-5}–$10^{-1}\ mol\ l^{-1}$. For H_2O_2 radiolytic production, the cell is filled with aerated deionized water and the UO_2/H_2O interface is irradiated to produce H_2O_2 concentrations in the range 5×10^{-4}–$7 \times 10^{-3}\ mol\ l^{-1}$.

The interfaces are irradiated by a He^{2+} ion beam delivered by the cyclotron at CERI-CNRS, Orléans (France). The beam at its source has a 45 MeV energy. After extraction from the cyclotron, the beam travels in air through a collimator and strikes the back face of the UO_2 disc that is mounted in the leaching cell. After passing through the UO_2 disc, the beam emerges from UO_2 into water with an energy that depends on the disc thickness. More details on the irradiation procedure are given elsewhere [11–13]. In the present work, due to the narrow dispersion of the disc thickness, the energy at the UO_2/water interfaces is $\sim 6.5 \pm 1.5$ MeV. This energy is comparable to the typical energy of alpha particles emitted by the alpha radioactive elements present in a spent nuclear fuel. The alpha-range in water at this energy calculated using TRIM98 code [23] is equal to about 37 μm.

Before starting the leaching sequences in presence of added or radiolytically produced H_2O_2, the UO_2 surfaces are pre-leached with aerated deionized water during a cycle of sequential dissolutions of 1 h each. This pre-leaching aims to reach a quasi-steady state level of the uranium release in aerated deionized water to which the uranium release over the first hour in presence of H_2O_2 can be compared.

During the leaching experiments in presence of added or radiolytically produced H_2O_2, either one continuous leaching or several sequential leachings are performed. For each continuous or sequential experiment, a new UO_2 disc and a fresh solution are used. At the end of each leaching, the solution is collected for characterisation and, for sequential leachings, replaced with a fresh solution. At the end of each experiment, the disc is dismounted for characterisation.

For H_2O_2 addition, the duration of the continuous leachings varies between 0.25 h and 1230 h. The number of sequential leachings is generally about 5 or 6 and the duration of each leaching is 1 h.

The fluxes used to produce radiolytically H_2O_2 are the same for the continuous and sequential leaching experiments, 3.3×10^{11} He^{2+} cm^{-2} s^{-1}. For the continuous leachings under irradiation, the duration varies from 1 to 6 h. Longer durations are impossible due to the management of the beam time at the CERI-cyclotron (CNRS-Orléans). For the sequential leachings under irradiation, two discs are irradiated several times at the same dates and a third disc at different dates. Between each irradiation, the cell is emptied and refilled with fresh water. The leaching time under irradiation that is cumulated is 5 h, corresponding to 5×1 h irradiations, for the two first discs and 16.5 h, corresponding to 2×0.25 h; 1×0.5 h; 12×1 h; 1×1.5 h; 1 h $\times$ 2 h irradiations, for the third disc. Between the irradiation sequences performed at different dates, the disc between the sequences is kept in a dry Ar atmosphere.

In the present experiments, the number of used discs is 20 and 10 for leachings using H_2O_2 addition and radiolytic production, respectively. The corresponding number of collected leachates including the pre-leachates is 120 and 49.

2.3. Analysis and characterisation

The total uranium concentration in each leachate is determined by inductively coupled plasma-mass spectrometry (ICP-MS) after acidification of the solutions to dissolve any colloid of uranium compounds that could have been formed during the leaching. The concentration of hydrogen peroxide either added or radiolytically produced is measured by the Ghormley method [24,25]. The H_2O_2 detection limit is 2×10^{-6} mol l^{-1}.

To determine the corrosion kinetic of UO_2, the altered layers are analysed by Rutherford backscattering spectrometry using $^4He^{2+}$ ions of 3.085 MeV at the Aramis facility of the CSNSM in Orsay. The RBS spectra are analysed with the RUMP computer code [26]. The microstructure at the UO_2 surface is also characterized by optical microscopy, scanning electron microscopy (SEM) and in the near surface layer by grazing X-ray diffractometry (XRD) before and after the leaching experiments. SEM observations are performed at DSM/DRECAM/LPS (CEA-Saclay) and XRD patterns are obtained at DEN/DMN/SRMA/LMS (CEA-Saclay).

3. Uranium release and acidity variation in presence of hydrogen peroxide

3.1. Pre-leaching in aerated deionized water

In our experimental conditions, the uranium release decreases as the number of sequential dissolution increases. It becomes quasi-constant after about four dissolutions. It has then the low value ~ 0.5 μg l^{-1}, corresponding to an average U release rate in volume per 1 h of ~ 0.5 μg l^{-1} h^{-1}. After normalisation to the S/V ratio (S; geometrical 6 mm diameter leached surface, V: 10 ml leaching volume), the release rate is equal to 1.8×10^{-2} μg cm^{-2} h^{-1}.

3.2. Addition of hydrogen peroxide

As concern H_2O_2 addition, Fig. 1 shows that the variation of the uranium mass release as a function of leaching time depends on the H_2O_2 concentration added in deionized water. For instance, one can compare the effects of 10^{-3} and 10^{-1} mol l^{-1} addition. In both cases, two different stages can be clearly distinguished. First, the uranium mass release increases rapidly. Then, the uranium mass release ceases to evolve as a function of the leaching time. The difference is that the saturation takes place at least four times faster for 10^{-1} mol l^{-1}

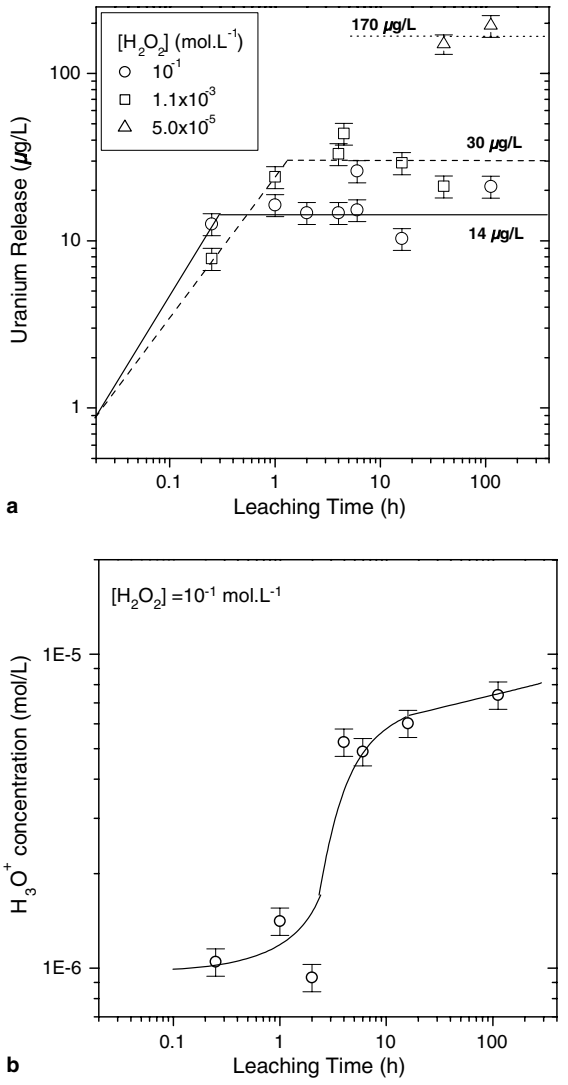

Fig. 1. Leaching experiments with H_2O_2 addition. (a) Uranium release as a function of leaching time and as a function of hydrogen peroxide concentration. (b) H_3O^+ concentration as a function of leaching time for 10^{-1} mol l^{-1} H_2O_2 addition.

than for 10^{-3} mol l^{-1} H_2O_2: in less than 15 mn instead of 1 h. This difference is however small compared to the variation of the added H_2O_2 concentration. The quasi-steady state is only reached four times, or more, faster as the H_2O_2 concentration increases by two orders of magnitude. Furthermore, as seen in Fig. 1, the saturation value of the U mass release depends weakly on the H_2O_2 concentration. This value decreases by only about one order of magnitude, from 170 to 14 µg l^{-1}, when the H_2O_2 concentration increases by four orders of magnitude, from 5×10^{-5} to 10^{-1} mol l^{-1}.

The acidity in the leachates increases as a function of leaching time. The increase depends weakly on the H_2O_2 concentration. For leaching time of about 100 h, the H_3O^+ concentration (pH) increases (decreases) from about 10^{-6} mol l^{-1} (6.0) to 10^{-5} mol l^{-1} (5.0) in the 10^{-3} and 10^{-1} mol l^{-1} H_2O_2 solution and to 2×10^{-5} mol l^{-1} (4.7) in the 5×10^{-5} mol l^{-1} H_2O_2 solution. The comparison of Fig. 1(a) and (b) for the 10^{-1} mol l^{-1} H_2O_2 solution shows the interesting property that the H_3O^+ concentration goes on increasing although the uranium release is stationary. The same property holds for the other solutions.

There is no significant variation of the hydrogen peroxide concentrations measured between the beginning and the end of the leaching experiments. This indicates that in the 5×10^{-5} mol l^{-1} H_2O_2 solution, the H_2O_2 consumption is at most of the order of 5×10^{-6} mol l^{-1}.

3.3. Radiolytic production of hydrogen peroxide

As shown in Fig. 2, the H_2O_2 concentration produced when UO_2/H_2O interfaces are under He^{2+} ion irradiation increases with the energy deposited in water. In our experimental conditions, a yield of H_2O_2 radiolytic production equal to 7.4×10^{-8} mol/J in Fig. 2 is obtained.

As illustrated in Fig. 3 for two different interfaces irradiated continuously in conditions that differ only by the irradiation time, the uranium release increases as a function of irradiation time. The H_2O_2 concentration produced after 4 h of irradiation at a flux of

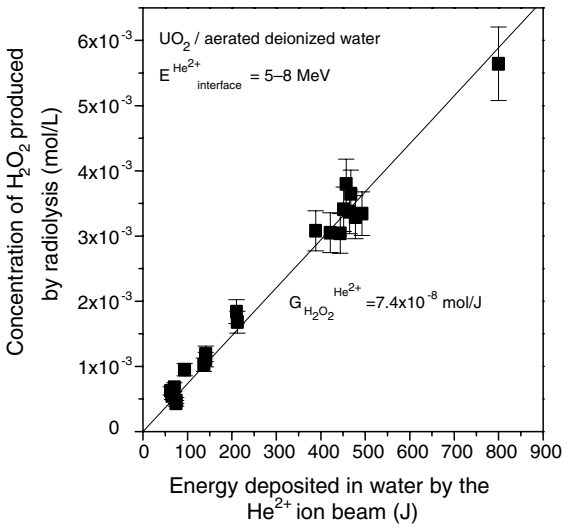

Fig. 2. Concentration of hydrogen peroxide produced at UO_2/H_2O interfaces under He^{2+} beam irradiation at high flux in the range ($0.33–14 \times 10^{11}$ He^{2+} cm^{-2} s^{-1}). The He^{2+} energy at the UO_2/H_2O interfaces varies between 5 and 8 MeV.

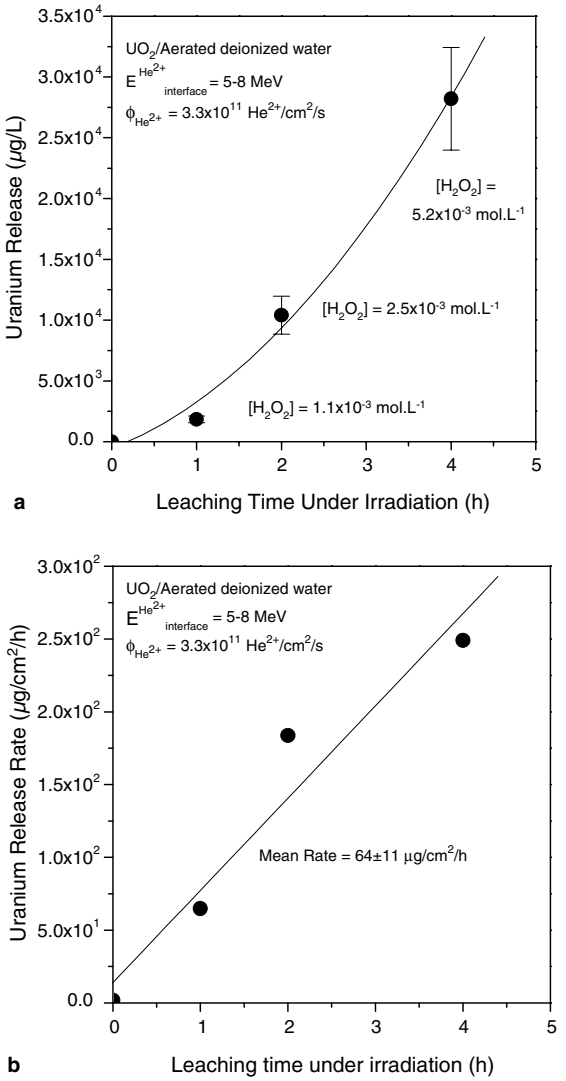

Fig. 3. UO_2/H_2O interfaces under He^{2+} beam irradiation at a flux of 3.3×10^{11} $He^{2+}\,cm^{-2}\,s^{-1}$. (a) Uranium release as a function of leaching time with the H_2O_2 concentration produced by water radiolysis indicated for each point. (b) Uranium release rate as a function of leaching time.

3.3×10^{11} $He^{2+}\,cm^{-2}\,s^{-1}$ reaches a value of 5.2×10^{-3} mol l^{-1}. The uranium release in Fig. 3 reaches then a value of about 2.8×10^{4} μg l^{-1}. Such a release is much higher than those measured (see Section 3.2) after 4 h of leaching by solutions where the added H_2O_2 concentration is about 5.2×10^{-3} mol l^{-1}.

The acidity in the solutions produced by He^{2+} irradiation of the UO_2/H_2O interfaces increases as a function of irradiation time. During 4 h of irradiation at a flux of 3.3×10^{11} $He^{2+}\,cm^{-2}\,s^{-1}$ where the H_2O_2 concentration produced by radiolysis increases to 5.2×10^{-3} mol l^{-1}, the H_3O^+ concentration (pH) increases (decreases) from 10^{-6} mol l^{-1} (6) to about 1.6×10^{-4} mol l^{-1} (3.8). This increase in acidity after 4 h of leaching under He^{2+} irradiation is much higher than those observed after ~100 h of leaching time in solutions where the added H_2O_2 concentrations fall in the range 5×10^{-5}–10^{-1} mol l^{-1}. The H_3O^+ concentration increases from about two orders of magnitude for 5.2×10^{-3} mol l^{-1} radiolytic production instead of one order of magnitude or less for 5×10^{-5}–10^{-1} mol l^{-1} addition.

4. Identification and growth kinetic of the alteration layer

4.1. XRD based identification of the alteration product

At the end of the leaching experiments performed in presence of added hydrogen peroxide, the UO_2 discs are dismounted from the leaching cells to be first analysed by X-ray diffraction and then observed by SEM. The leached faces are coated with a yellow deposit, macroscopically visible. The X-ray diffraction patterns with grazing incidence recorded on the leached faces show the formation of the tetrahydrated uranium peroxide called studtite $UO_2(O_2)\cdot4H_2O$ (Fig. 4(a)). After SEM observations or RBS characterisation, the XRD patterns correspond to a dehydrated uranium peroxide $UO_2(O_2)\cdot2H_2O$ (metastudtite, Fig. 4(b)). This transformation indicates a loss of water molecules in the vacuum of the SEM or RBS analysis chambers. The same compounds are identified on the faces of the UO_2 discs leached under He^{2+}-irradiation. Depending whether characterisation by XRD precedes or not those by SEM or RBS, the secondary phases observed are either studtite or metastudtite.

The morphology of studtite has similar aspects independently whether the growth takes place for H_2O_2 addition or radiolytic production. In both cases, it appears to grow as a finely divided solid. It is interesting to follow the evolution of the morphology of the surface as its alteration progresses. Before leaching, the SEM images of the polished faces of a UO_2 disc have the typical aspect shown in Fig. 5(a). The surface appears to be smooth with well visible grain boundaries. The grains have an average size of about 10 μm. After 16 h of leaching with a 10^{-1} mol l^{-1} H_2O_2 solution, the altered UO_2 surface in Fig. 5(b) is covered homogeneously by a alteration product that displays microcracks. The original grain boundary structure of the UO_2 disc has disappeared. After about 40 times longer leaching time, about 27.3 d (676 h) instead of 0.66 d (16 h), Fig. 5(c) shows that the studtite layer develops and takes a well defined structure. It appears as closely packed crystalline fibres that grow with a parallel orientation perpendicular to the UO_2 surface. After leaching under He^{2+}-irradiation at the

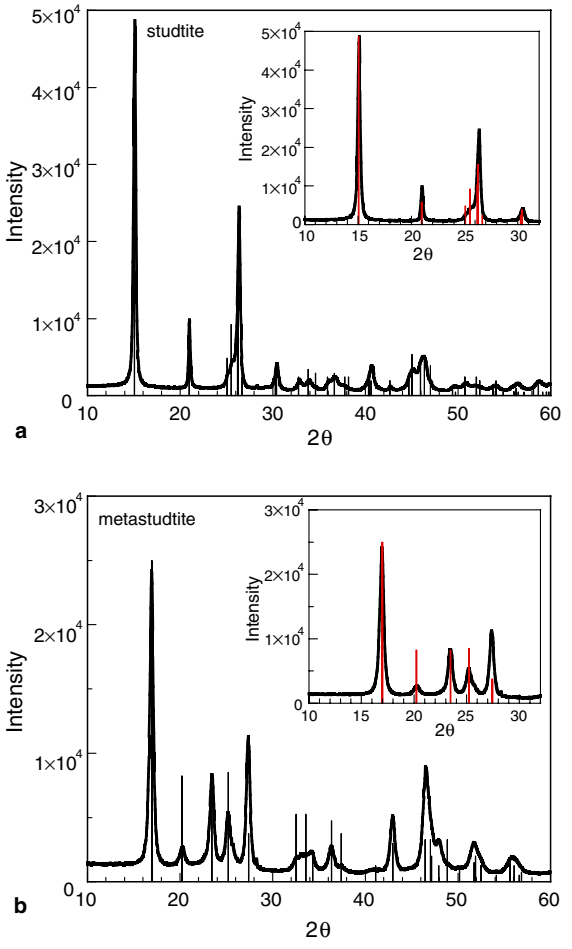

Fig. 4. X-ray diffraction patterns obtained with a grazing incidence of 1° and with the wavelength $\lambda_{CuK\alpha 1} = 1.54060$ Å on altered UO_2 discs after leaching with either H_2O_2 addition or radiolytic production under He^{2+}-beam irradiation. (a) Studtite, (b) metastudtite produced after dehydration of studtite in vacuum; the insets show details for the low diffraction angles.

high flux of 3.3×10^{11} He^{2+} cm^{-2} s^{-1}, the alteration product appears as closely packed bundles of randomly oriented crystalline rods (Fig. 5(d) and (e)). There is apparently no preferential direction of growth in the case of leaching under irradiation.

It is interesting to notice that the surface beyond the sealing joint of the leaching cell has a similar appearance to that before leaching. It is consequently unaltered. Another point worth mentioning is the mechanical weakness of the altered layer. When the thickness of studtite is sufficiently high (> several μm), this alteration product is easily removed from the UO_2 surface by scratching and falls into a loose yellow powder. After 1230 h of leaching time with 10^{-1} mol l^{-1} of H_2O_2, the UO_2 disc is totally disintegrated into a yellow powder.

4.2. Growth kinetic of the alteration layer: a RBS based determination

Fig. 6 shows the typical evolution of the RBS spectra recorded for different UO_2 discs as leaching time in presence of H_2O_2 addition or radiolytic production increases. Fig. 6 displays the normalized RBS yields in a range of channels corresponding only to the high energy range of backscattered $^4He^{2+}$ ions. This high energy part of the RBS spectra corresponds to $^4He^{2+}$ ions that are backscattered by uranium atoms in the near-surface region. As illustrated in Fig. 6 for 1 h, 4 h and 16 h leaching after 0.1 mol l^{-1} H_2O_2 addition, leaching induces a decrease of the uranium backscattering yield in a thin layer beyond the surface of the discs. This layer extends as leaching time increases and, finally, becomes so thick that, after 16 h of leaching, the remaining UO_2 is no longer reached by the analysis $^4He^{2+}$-ion beam.

The comparison of the backscattering yields at the surface in Fig. 6 after 1 h, and 4 h of leaching in presence of 0.1 mol l^{-1} H_2O_2 addition shows that the composition of the altered layer at the surface is close to that of the layer formed after 16 h of leaching. The decrease in the uranium backscattering yield indicates that the density of uranium atoms in the near surface region decreases. By correlating this decrease to the formation of altered layers of hydrated uranium peroxide at the disc surface, $UO_2(O_2)$–nH_2O, we conclude that this decrease corresponds to the incorporation of O and H at and in the near-surface of the discs. The thickness of the altered layer is deduced from the energy range where the uranium backscattered yield varies. The yield variation depends on the density of oxygen, hydrogen and uranium atoms in the altered layer.

The thickness of the alteration layer is calculated by fitting the RBS spectra with the RUMP code in a model where the atomic composition of the altered layer is assumed to vary continuously as a function of depth from the composition at the extreme surface, $UO_2(O_2)$–nH_2O, to the UO_2 composition. In a first sublayer, the composition is given by $UO_2(O_2)$–nH_2O and depends only of n. In a second one, the composition is given by UO_x with $2 < x < 4$. Details on the fitting procedure are given in Appendix A.

In all the leached discs, the composition of the extreme surface is close to $UO_2(O_2)$–nH_2O, with $0.4 < n < 1.6$, indicating an uranium peroxide compound partially dehydrated. As shown in Fig. 7(a), after addition of H_2O_2 in the solutions, the calculated thickness of the alteration layer increases both with leaching time and H_2O_2 concentration. The variation of thickness with leaching-time is linear for the H_2O_2 concentration range between 10^{-1} and 10^{-3} mol l^{-1}. The slopes of the straight lines give the growth rates of the alteration

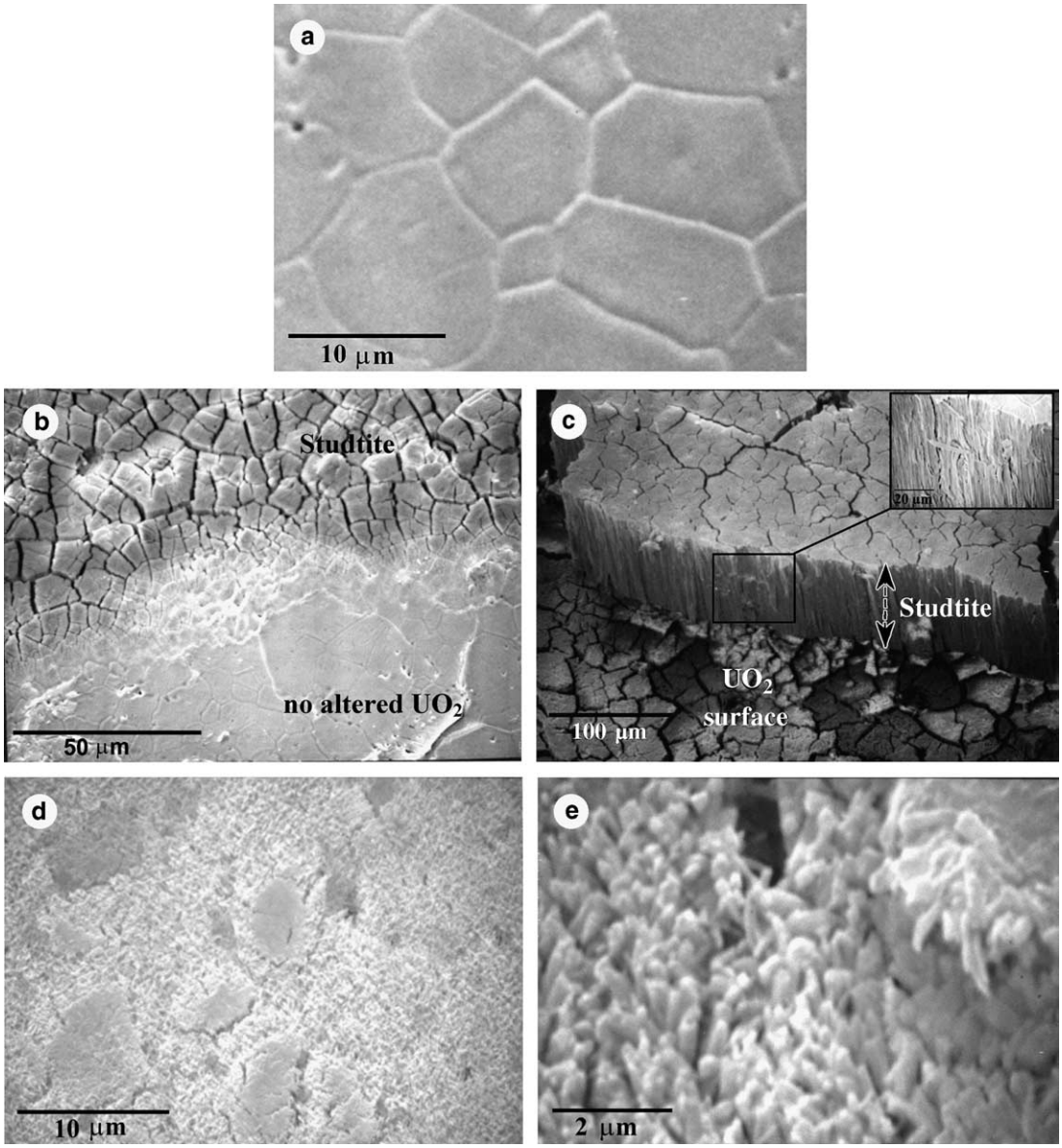

Fig. 5. Scanning electron microscopy characterisation of UO_2 surfaces before and after leaching in aerated deionised water with H_2O_2 addition or radiolytic production under He^{2+}-beam irradiation. (a) Before leaching. (b and c) After leaching with 10^{-1} mol l^{-1} H_2O_2 addition during (b) 16 h and (c) 676 h; the inset shows a detail of closely packed fibres of studtite with a parallel orientation and growing in a direction perpendicular to the UO_2 surface. (d and e) Closely packed bundles of randomly rod-shaped crystals of studtite after leaching under He^{2+}-beam irradiation with a flux of 3.3×10^{11} He^{2+} cm^{-2} s^{-1}.

layer. Fig. 7(b) shows that the growth rate increases with increasing added H_2O_2 concentration. It varies in Fig. 7(b) by a factor 10, from $\sim 25 \pm 2$ to 200 ± 10 nm h^{-1}, when the H_2O_2 concentration increases from 1.1×10^{-3} to 10^{-1} mol l^{-1}. From a threshold H_2O_2 concentration of $\sim 6 \times 10^{-4}$ mol l^{-1}, an empirical equation can adjust the variation of the growth rates with the added H_2O_2 concentration (Fig. 7(b)). For $[H_2O_2] \geqslant 6 \times 10^{-4}$ mol l^{-1}, the growth rate per hour, GR, is given by:

$$\mathrm{GR}\ (\mathrm{nm\ h^{-1}}) = 295 + 92 \log([H_2O_2]\ (\mathrm{mol\ l^{-1}})) \quad (1)$$

or, after normalisation to the leached surface:

$$\mathrm{GR}(\mathrm{nm\ cm^{-2}\ h^{-1}}) = 1042 + 325 \log([H_2O_2]\ (\mathrm{mol\ l^{-1}})). \quad (2)$$

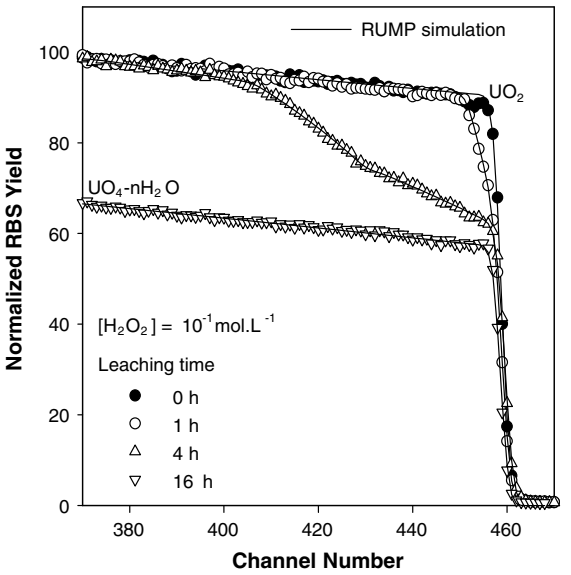

Fig. 6. Rutherford backscattering spectra for UO_2 discs before and after 1, 4 and 16 h leaching with 10^{-1} mol l^{-1} H_2O_2 addition and comparison with RUMP simulation.

Below 6×10^{-4} mol l^{-1}, the growth rate is low and is of the order of a few nanometers per hour. Experiments are underway to determine more precisely the behaviour of the growth rates in this range of low H_2O_2 concentrations.

The RBS spectra for the UO_2 discs leached under He^{2+} beam irradiation have the same features as those obtained on the discs leached in presence of added H_2O_2 and are analysed in the same way. The thickness of the alteration layer increases as a function of irradiation time. Fig. 8 shows that the growth rate however decreases as a function of irradiation time although the concentration of H_2O_2 produced by radiolysis increases. This tendency is true for the two discs that have undergone a unique continuous irradiation as well as for the three discs that have been submitted to a sequence of several similar irradiations and for which, for each irradiation, the cell is refilled with fresh deionized water. During each irradiation, the H_2O_2 concentration, produced by radiolysis at the UO_2/H_2O under He^{2+} beam under irradiation, has an average value of $(1.3 \pm 0.5) \times 10^{-3}$ mol l^{-1} h^{-1}. As seen in Fig. 8, the average growth rates determined at a given flux during sequential and continuous irradiations are of the same order for duration that are comparable. For example, the rate has a value of about 68 ± 14 nm h^{-1} for a unique run where the H_2O_2 concentration produced by 4 h radiolysis is 5.2×10^{-3} mol l^{-1}. The value is 78 ± 7 nm h^{-1} for 5×1 h runs where the average H_2O_2 concentration produced by 1 h radiolysis in each run is about 1.2×10^{-3} mol l^{-1}.

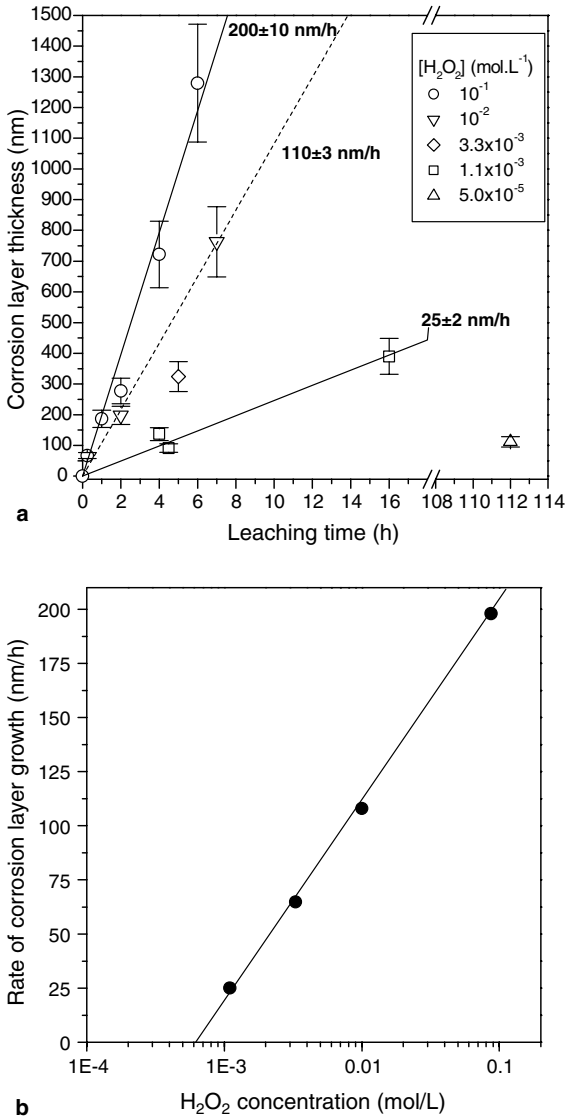

Fig. 7. Alteration of UO_2 discs after leaching in aerated deionised water with H_2O_2 addition. (a) Thickness of the corrosion layer as a function of leaching time for H_2O_2 concentration in the range 5×10^{-5}–10^{-1} mol l^{-1}. (b) Growth rate of the corrosion layer as a function of hydrogen peroxide concentration.

5. Ageing of $UO_2/H_2O[H_2O_2]$ aerated interface for H_2O_2 addition

5.1. UO_2 corrosion induced by H_2O_2 addition in deionized water

During the leaching with added H_2O_2, a yellow product occurs on the UO_2 disc surfaces. It is identified by X-ray diffraction as to be the tetrahydrated uranium

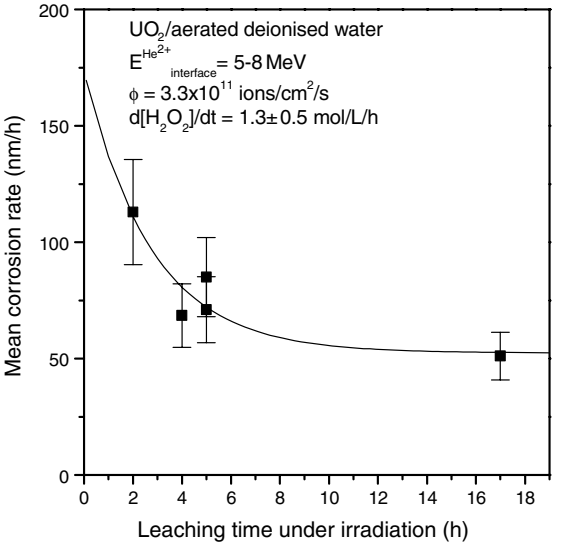

Fig. 8. Growth rate of the corrosion layer as a function of leaching time during leaching experiments under He^{2+}-beam irradiation with a flux of 3.3×10^{11} He^{2+} cm^{-2} s^{-1}.

peroxide studtite $UO_2(O_2)$–$4H_2O$. It has a monoclinic structure and the unit-cell dimensions are $a=$ 1.185 nm, $b=0.678$ nm, $c=0.425$ nm and $\beta=93°37'$, with a density of 3.64 g cm^{-3} [27–29]. The present work shows that the compound can be easily dehydrated under vacuum when it is examined with an electron or He^{2+} beam. The layer is transformed into the uranium peroxide dehydrate $UO_2(O_2)$–$2H_2O$ called metastudtite. Its structure is orthorhombic with cell dimensions of $a=0.650$ nm, $b=0.878$ nm, $c=0.421$ nm, and a density of 4.67 g cm^{-3} [27,28]. In both peroxides, the uranium has the oxidation degree, U(VI), and three different types of oxygen bonds coexist [30–33]. The conclusion is that H_2O_2 addition to water induces a corrosion process where U(IV) is transformed into U(VI). The formation of uranium peroxides on UO_2 has been earlier mentioned in dissolution experiments performed with H_2O_2 added to sulfate aqueous solutions of various pH [15,17] or more recently to deionized water [11–13,21,22].

To our knowledge, the present work reports the first investigation where the growth rate of the corrosion layer on UO_2 is systematically determined as a function of the concentration of added H_2O_2 in deionized water. The corrosion layer thickness varies linearly with leaching-time for all the H_2O_2 concentrations. The growth rate increases with the H_2O_2 concentration. It is however a weak logarithmic dependency (see Section 4.2). The growth rate increases by only one order of magnitude from about 10 to 200 nm h^{-1} (35 to 707 nm cm^{-2} h^{-1}) when the added H_2O_2 concentration increases by four orders of magnitude from 5×10^{-5} to 10^{-1} mol l^{-1}. For a studtite density of 3.46 g cm^{-3}, it follows that the studtite forms at rates in the range $(9.5–190)\times10^{-8}$ mol m^{-2} s^{-1}. Once a first layer of the UO_2 disc is transformed into $UO_2(O_2)$–$4H_2O$, the transformation goes on until the whole UO_2 is transformed. The formation of the studtite layer is unable to protect UO_2 from further transformation.

It is interesting to compare the layer growth rate obtained here from RBS to the growth rate of the small crystalline rods that compose studtite and obtained in [34] from AFM. For $[H_2O_2]=5\times10^{-4}$ mol l^{-1}, the authors report data showing that the growth rate drops from 0.49 nm/h to 0.2 nm/h as the studtite formation progresses. These values are obtained in deaerated conditions on as-polished UO_2 discs. They are about two orders of magnitude lower than the layer growth values, 10 and 25 nm/h, obtained here in aerated conditions on annealed UO_2 discs for H_2O_2 concentrations of 5×10^{-5} and 1.1×10^{-3} mol l^{-1}, respectively. After normalisation to the same specific surface area as in our experiments, the ratio S/V for the deaerated conditions is 1.5×10^{-2} m^{-1}. It is much lower than the value 2.8 m^{-1} used here for the aerated conditions. In addition to the absence of oxygen that can lower the rate of formation of studtite, this difference can also affect the growth rate of studtite.

5.2. U release as a function of UO_2 leaching time in presence of H_2O_2 addition in deionized water

In the present work, the U mass in the solutions is determined after acidification. It takes into account the U mass dissolved in the solution as well as the U mass that may exist under the form of colloids or small precipitates in the solutions. Consequently, it is referred below as the total U mass in solution. As mentioned in Section 2, the effect of H_2O_2 addition is investigated in this work once the total U mass release rate per hour in deionized water has reached a constant value. In these conditions, it is found that the total U mass release rate during the first dissolution in presence of H_2O_2 addition varies as function of leaching time. For every H_2O_2 concentration used in this work, the same evolution is observed. The total U mass release rate in solution decreases and tends towards zero as leaching time increases. The saturation value of the total U release and the leaching time necessary to reach the saturation are both dependent on the added H_2O_2 concentration. Both quantities decrease weakly with increasing H_2O_2 concentrations. The decrease is less than an order of magnitude when the H_2O_2 concentration increases by two orders of magnitude in the range 10^{-3}–10^{-1} mol l^{-1}.

The effect of the H_2O_2 addition on the dissolution of UO_2 in presence of aqueous solutions of various compositions has been investigated in a few earlier works

[14–22]. The main focus is generally on the measurements of the release rates in the first stage where the uranium release increases as a function of leaching time. The second stage at longer leaching time, where there is saturation of the uranium release and an apparent release rate of zero, is rarely investigated or even mentioned. A direct comparison between the release rates determined in the previous studies and ours is meaningless because they are determined for a wide range of different experimental conditions. The leaching times, the ratio S/V of the UO_2 surface to the leaching volume, the solution composition, acidity and redox conditions, such as aerated versus deaerated leachings, differ strongly from one study to the other. The effect of H_2O_2 on the U release rates at the beginning of leaching depends strongly on the solution composition, acidity and redox conditions. The comparison of the different investigations show that the release rates can vary by two or three order of magnitudes. As concerns the values of the U release after long leaching times of UO_2 pellets in deionized water, it has been recently reported results showing the same trends as ours [21]. The U release decreases with increasing H_2O_2 concentrations. After 1000 h of leaching in 10 ml, the decrease is about an order of magnitude, from about 4760 μg/l to 380 μg/l, when the H_2O_2 concentration increases by three orders of magnitude from 10^{-5} to 10^{-2} mol l^{-1} [21].

6. U and H_3O^+ release as a function of UO_2 corrosion for H_2O_2 addition

6.1. U release and UO_2 corrosion for H_2O_2 addition in deionized water: correlation

For every H_2O_2 concentration used in this work, the comparison between the total U mass release rate in solution and the growth rate of the corrosion layer shows that they vary independently as a function of leaching time. The release decreases and tends towards zero whereas the growth rate of the corrosion layer remains constant as leaching time increases. This interface behaviour indicates that the growth of the secondary phase slows down the total U release. A similar conclusion can be drawn from sequential leaching experiments, $n \times 1$ h, performed with the same leaching cell. As earlier reported [11], the total U release rate per hour decreases as the number of sequential dissolutions, $n \times 1$ h, in aerated added 10^{-3} mol l^{-1} H_2O_2 solution increases. The U valence state being U(VI) in studtite, it is reasonable to assume that the growth of the corrosion layer slows down the release of the U(VI) valence state. The consequence is that most of the U(IV) valence state transformed into the U(VI) valence state remains in the solid. The interface has thus the interesting property that the UO_2 corrosion rate becomes equal to the growth rate of the corrosion layer as leaching time increases. Furthermore, the property that studtite formation decreases the release of the valence state U(VI) indicates that studtite is stable in water in presence of H_2O_2.

When H_2O_2 is added to deionized water, the comparison between the U mass release rates in absence and presence of H_2O_2 shows that H_2O_2 addition in our experimental conditions enhances strongly the total U mass release rate. For example, for 10^{-3} and 10^{-1} M H_2O_2 addition (Fig. 1), the rates over the first quarter of dissolution are respectively about $\geqslant 15.6$ and $\geqslant 25.2$ times higher than the rate over the first hour of dissolution, 0.5 μg l^{-1} h^{-1}, measured in absence of H_2O_2 (see Section 2). This increase indicates that H_2O_2 addition modifies the reactions undergone by U species either at the altered disc surface and/or in solution.

As concern the surface, the transformation of UO_2 into studtite during the first quarter of dissolution indicates that an oxidation process takes place. Little information is available about the mechanism of this transformation that is rarely discussed in previous works [2–8,15]. It is generally accepted that the uranium mass loss rate from uranium oxide is strongly dependent on the surface oxidation, UO_{2+x} [35]. The dissolution rate of uranium from an UO_{2+x} surface is generally considered much higher for its valence state U(VI) than in its valence state U(IV). The increase in the total uranium release induced by H_2O_2 addition during the first quarter of dissolution may partly reflect the oxidation process that is involved in the production of studtite on the UO_2 disc surface.

As concern the reactions in solutions, the complexation and precipitation reactions that may occur between uranyl ions and H_2O_2 can also enhance the total U release in solution. The complexation reactions that are reported by some authors [36] lead to the formation of $UO_2(O_2)$ and $UO_2(O_2)^{2-}$ ions via the reactions:

$$UO_2^{2+} + O_2^{2-} > UO_2(O_2) \quad \text{(R1)}$$

$$UO_2^{2+} + 2O_2^{2-} > UO_2(O_2)_2^{2-} \quad \text{(R2)}$$

with, for the reaction constants $\beta_{ij} = \frac{[U_iL_j]}{[U]^i[L]^j}$, the values $\mathrm{Log}\,\beta_{11}^{(R1)} = 32.04$ and $\mathrm{Log}\,\beta_{12}^{(R2)} = 60.15$. The precipitation reactions lead to the formation of studtite at room temperature according to the reaction [27–29]:

$$UO_2^{2+} + H_2O_2 \rightarrow UO_2(O_2)_s + 2H^+ \quad \text{(R3)}$$

The solubility constant $K = ([UO_2^{2+}][H_2O_2]/[H^+]^2)$ is reported to be 1.3×10^{-3} in the temperature range 25–27 °C [37, and refs. herein] and more recently (1.32–1.38) at 25 °C [38]. This relation is valid when precipitation takes place in pure solutions. In the present experimental conditions, the studtite layer is formed on a UO_2 disc surface initially immersed in the solution.

The relation (R3) can however be used to estimate the quantity of uranyl ions that needs to be added to start studtite precipitation in solutions that contain the same H_2O_2 and H_3O^+ concentrations as the leachates. After 1 h and 112 h of aerated leaching in presence of 10^{-1} mol l^{-1} H_2O_2 addition (Fig. 1), the H_2O_2 and H_3O^+ concentrations are such that the solubility limit is reached for concentrations of uranyl ions that are about 2.5×10^{-14} and 8×10^{-13} mol l^{-1}, respectively. These calculated concentrations are about six or five orders of magnitude lower than the saturated U concentration of $\approx5.9\times10^{-8}$ mol l^{-1} measured in the corresponding leachates. The comparison between the calculated and experimental values suggests consequently that precipitation takes place in the leachates. It follows that, in addition to the oxidation process occurring at the UO_2 disc surface and to the complexation reactions, the formation of tiny studtite colloids by precipitation may contribute to enhance the U release when H_2O_2 is added. This justifies the experimental procedure used to measure the U amount in solutions (see Section 2.3). The solutions are acidified before performing ICP-MS measurements to dissolve any type of U containing colloids.

The complexation and precipitation reactions induced by H_2O_2 in solutions are expected to increase the total U release as a function of increasing H_2O_2 concentration. The opposite behaviour is observed in the present experiments for the saturation values reached by the U release as leaching time increases. The saturation values decrease as a function of increasing H_2O_2 concentration. It seems therefore unlikely that the reactions in solutions determine the saturation values of the U release. It is proposed here that they are determined by the U release properties of the surfaces that appear while the transformation from UO_2 to $UO_2(O_2)$–$4H_2O$ progresses. We have seen above that, in presence of H_2O_2, the release of the U(VI) valence state seems to be blocked from studtite surface but occur rather easily from UO_{2+x} surface. The time spent in surface states that favour U release decreases when the growth rate increases. The consequence is that faster the growth of a studtite surface is, lower the U saturation value is. This is indeed the observed experimental trend. For example, the growth rates of the corrosion layer is higher for 10^{-1} mol l^{-1} than for 10^{-3} mol l^{-1} H_2O_2 addition whereas the U saturation value is lower for 10^{-1} mol l^{-1} than for 10^{-3} mol l^{-1}.

6.2. Acidification and UO_2 corrosion for H_2O_2 addition in aerated deionized water

Another interesting property induced by the leaching of the UO_2/H_2O interface with added H_2O_2 is that the acidity goes on increasing as leaching time increases. The question is whether this increase results from reactions in solutions or/and at the $UO_2/H_2O([H_2O_2])$ interface. Some of the reactions in solutions that can be candidates for the control of the acidity in the aerated leachates are the hydrolysis reactions of uranyl ions and their derivatives, the formation of U complexes with the peroxide ions or the carbonates present in aerated solutions. The concentrations of uranyl ions and of their derivatives soluble in the leachates are here unknown. They are equal or lower than the total U concentrations that are measured by ICP-MS after acidification of the leachates. A calculation shows that, for values equal or higher than the U concentration in the leachates, the hydrolysis reactions result in an acidity that is lower than measured. When reactions with peroxide ions and carbonates are also considered, the calculated $[H_3O^+]$ concentrations remain below the measured values. For instance, for $([U],\ [H_2O_2]) = (10^{-5}, 10^{-3})$ mol l^{-1} and $p_{CO_2} = 3.4\times10^{-4}$ atm, the calculated value is $[H_3O^+]_{cal} = 2.85\times10^{-6}$ mol l^{-1}. Consequently, other reactions are responsible for the acidification of the solutions. Among the reactions that can be considered is the precipitation reaction (R3) (see Section 6.1). The formation in solution of tiny studtite colloids via this reaction can result in an increase of the solution acidity. However, contrary to the acidity that increases as a function of leaching time, the total U amount in the leachates, and, consequently, the precipitated part in tiny colloids, tend towards a constant value. It seems therefore unlikely that the precipitation reaction (R3) contributes to the increase in acidity that is observed after long leaching times. The conclusion is that reactions at the $UO_2/H_2O([H_2O_2])$ interface rather than in the solution need to be considered.

A process occurring at the interface when the acidity increases is the growth of the studtite layer on the UO_2 disc. The correlation between the increase in acidity and the growth of the studtite suggests that the H_3O^+ production be partly related to the transformation of uranium oxide into studtite. In the present work, the disc alteration has the two properties that (i) the altered disc surface presents an etch pattern and (ii) the layer thickness increases linearly. According to literature, these two properties can be considered as indicative of a corrosion process controlled by a reaction at the interface ((i) [40], (ii) [39]). One possibility is that the UO_2 surface acts as a nucleation site for precipitation. If the UO_2 surface has indeed this role, the reaction precipitation at the surface produces H_3O^+ and, consequently, the increase in acidity can be partly controlled by the growth of the studtite layer. The layer grows as closely packed crystalline rods with a more or less well defined orientation depending whether its growth is induced by hydrogen peroxide addition or radiolytic production. This indicates that heterogeneous nucleation takes place. The rod disorientation observed when the hydrogen peroxide is radiolytically produced can have its origin in the formation of

tiny H_2 gas bubbles that stick more or less on the surface during the interface irradiation. Work under progress shows that the measurements of the electrochemical properties of the interface can be hindered after a while under irradiation by such a process.

6.3. Summary

In summary, for the leaching experiments with H_2O_2 addition, the corrosion and release processes can be divided into two main stages:

- a first stage where the U release rate is quasi-constant as a function of time and much higher than in deionized water. The surface is oxidised and studtite starts to grow on the surface.
- a second stage where the total U release ceases to evolve whereas the studtite layer on the disc goes on growing with a constant rate depending on the added H_2O_2 concentration. A continuous release of H_3O^+ ions seems to be correlated to the growth of the studtite layer.

The comparison between the total U releases produced in continuous or sequential leaching experiments suggests that the net U release from the disc surface decreases as the studtite layer grows. The valence state U(VI) in studtite seems to be stabilised against dissolution.

7. Ageing of $UO_2/H_2O[H_2O_2]$ aerated interface: radiolytic versus added H_2O_2

7.1. UO_2 corrosion and U release for H_2O_2 radiolytic production in deionized water

For the leaching experiments where H_2O_2 is produced by radiolysis at the UO_2 surface under He^{2+} irradiation at a flux of 3.3×10^{11} He^{2+} cm^{-2} s^{-1}, the H_2O_2 concentration increases continuously during the leaching process. The UO_2 discs are altered and studtite grows during irradiation. As seen in Section 5.1, the formation of this compound indicates that a corrosion process takes place where the valence state U(IV) is oxidised to the valence state U(VI).

For continuous irradiation, the growth rate of the corrosion layer decreases as a function of leaching time. The decrease can reach values of about 40% during the first 4 h. For the sequential irradiation where the discs are irradiated several times in conditions that produce comparable H_2O_2 concentrations, the growth rates of the corrosion layer tend also to decrease as the cumulated irradiation time increases. The rate value is 78 ± 7 nm h^{-1} for the two discs that are irradiated five times during 1 h. It is only 51 ± 10 nm h^{-1} for the disc that is irradiated 16.5 h (2×0.25 h; 1×0.5 h; 12×1 h; 1×1.5 h; $1\text{ h}\times2$ h). The growth rate seems however to tend towards a constant limit as the cumulated irradiation time increases. This tendency suggests that the corrosion in the discs goes on progressing as cumulated irradiation times increases.

For the discs that are irradiated in the same flux conditions, the comparison of the growth rates of the corrosion layer shows that the growth rates determined for short unique irradiation times are higher than or comparable to those determined for longer cumulated irradiation times: 112 ± 22 and 68 ± 14 nm h^{-1} for 2 and 4 h of continuous irradiation instead of 78 ± 7 and 51 ± 10 nm h^{-1} for 5 h (5×1 h) and 16.5 h (2×0.25 h; 1×0.5 h; 12×1 h; 1×1.5 h; $1\text{ h}\times2$ h) of cumulated irradiation. This tendency confirms that the growth rate seems to tend towards a limit when the studtite layer grows under a given flux of He^{2+} ions.

The total uranium release and the acidity increase as a function of H_2O_2 production. There is no trend towards saturation at least during the first 5 h of irradiation where there is also no saturation in the H_2O_2 production. The total U release increases as a function of the radiolytically produced H_2O_2 according to the empirical relation:

$$[U]_{irr}\ (\text{mol}\,l^{-1}) = -2.27\times10^{-6} + 1.11\times10^{-4}[H_2O_2]_{irr}\ (\text{mol}\,l^{-1}) + 2.34[H_2O_2]^2_{irr}\ (\text{mol}\,l^{-1}).$$

The total U release rate has a quasi-constant value of 64 μg cm^{-2} h^{-1} (Fig. 3(b)). This rate remains quasi-constant although irradiation induces a corrosion process that transforms UO_2 into studtite. The comparison between this time dependency and that of the growth rate of the corrosion layer shows that these two quantities vary independently.

7.2. Solid and leachate evolution: difference between H_2O_2 addition and radiolytic production

This section compares the effects of H_2O_2 addition and radiolytic production on the evolution of $UO_2/H_2O[H_2O_2]$ interfaces and show that the behaviour of the interfaces differ.

When H_2O_2 is added in deionized water, the $UO_2/H_2O[H_2O_2]$ interface starts to evolve at a constant value of H_2O_2 concentration. When H_2O_2 is radiolytically produced in deionized water at the interfaces under He^{2+} beam, the interface starts to evolve in presence of H_2O_2 concentrations that increase with irradiation time. Furthermore, other radiolytic chemical species than H_2O_2 are produced at the interface. Depending whether they react or not with the UO_2 surface, they can also induce an evolution of the surface. The comparison of

the behaviours of UO_2/H_2O interfaces in both situations show that two properties that differ significantly are the evolutions of the release and growth rates as a function of leaching time. In both cases, the corrosion process however transforms UO_2 into a secondary phase that is identified as studtite. In both cases, the layer morphology appears as a loose structure formed by closed bundles of thin rods.

Under irradiation, the total U release rate remains quasi-constant although the leaching time and H_2O_2 concentration reach values that, for H_2O_2 addition experiments, correspond to values where the release rate has already decreased to zero. Let us consider the following example. In Fig. 3, the total U release under irradiation is still increasing after 1 h. The H_2O_2 concentration is produced at the constant rate of $\approx 3.3 \pm 0.3 \times 10^{-7}$ mol l^{-1} s^{-1} (Fig. 3) and, after 1 h, reaches the value $\approx 1.3 \times 10^{-3}$ mol l^{-1}. After 1 h of leaching at such added concentrations, Fig. 1 shows that the total U release has already reached a stationary value. Our conclusion is that the U release rate under irradiation is controlled by other processes than those controlling it in presence of H_2O_2 addition. The redox conditions under irradiation are strongly modified due to the production of strong transient oxidant ($HO^{\bullet}$, $O^{\bullet -}$, HO_2^-, $O_2^{\bullet -}$, H_3O^+, H_2O_2, O_2) or reductant ($e_{aq}^{\bullet -}$, $H^{\bullet}$, H_2, H_2O_2) radiolytic species. This may be the origin of the striking difference in the release amounts and rates as a function of leaching time between irradiation and addition.

The growth rates at the beginning of the leaching seem to be higher under irradiation than those that can be achieved by low addition of H_2O_2 concentrations. As leaching time under irradiation increases and that radiolysis produces H_2O_2 concentrations in the range 10^{-3}–10^{-2} mol l^{-1}, the growth rates seem to become comparable to those obtained for the addition of H_2O_2 concentrations equal to those produced by radiolysis. For example, the average growth rate after 2 h of irradiation has a value 112 ± 22 nm h^{-1} for H_2O_2 concentrations increasing from 0 up to ≈ 1.3 mol l^{-1} during the first hour and up to ≈ 2.5 mol l^{-1} during the second hour. It is higher than the growth rates corresponding to, respectively, 1.3 and 2.5×10^{-3} mol l^{-1} H_2O_2 addition. The average growth rate after 4 h of irradiation has a value 68 ± 14 nm h^{-1}. This value falls in the range of rates 60–70 nm h^{-1} that can be obtained by averaging the rates 30, 56, 71 and 83 nm h^{-1} equal to those induced by the addition of H_2O_2 concentrations comparable to those produced after 1 h, 2 h, 3 h and 4 h irradiation, respectively $(1.3, 2.5, 3.8, 5.2) \times 10^{-3}$ mol l^{-1}. It seems also that, as the cumulated irradiation time increases in a cycle where similar irradiations are repeated, the growth rate of the corrosion layer becomes close to that induced by the addition of the H_2O_2 concentration that is reproducibly produced in each irradiation. The presence of other radiolytic species than H_2O_2 seems to affect the growth process rather at the beginning than after a few hours of irradiation.

In summary, the evolution of the UO_2/H_2O interface induced by H_2O_2 radiolytic production results in specific properties of the U release and initial growth rate of the alteration layer that H_2O_2 addition is unable to reproduce. The nature of the corrosion product is however the same in both cases.

7.3. H_2O_2 consumption in UO_2 corrosion induced by H_2O_2 in aerated deionized water

The mechanisms of the transformation of uranium oxide into studtite and those of the studtite dissolution are rarely discussed in previous works [14–22,38] and little is known about them for H_2O_2 addition as well as radiolytic production. Recent calculations of enthalpy formation suggest that studtite, $UO_2(O_2)$–$4H_2O$, relative to UO_3 is stable in presence of H_2O_2 [38]. Another enthalpy formation calculation suggests that studtite instead of dehydrtated shoepite, $UO_3(H_2O)_{0.8}$, forms when very low H_2O_2 concentrations, $\sim 1.1 \times 10^{-14}$ mol l^{-1}, are added to deionized water [38].

To calculate the consumption of H_2O_2 as a function of leaching time in our experimental conditions, we assume that the reaction (R4) takes place:

$$UO_{2_s} + 2H_2O_2 \rightarrow UO_2(O_2)_s + 2H_2O \qquad (R4)$$

Two moles of H_2O_2 are used to transform one mole of UO_2 into studtite. Let us calculate the H_2O_2 concentration that is needed to transform a UO_2 layer of 1 nm. For a UO_2 disc, of typically 0.15 g and thickness 270 μm in our study, the number of UO_2 moles per nm is 2.0×10^{-9} mol nm^{-1}. According to reaction (R4), the number of H_2O_2 moles per nm required for the transformation of a UO_2 disc layer into studtite is then 4.0×10^{-9} mol nm^{-1}. In the assumption that all the H_2O moles in solution contributes to the transformation, the addition of a H_2O_2 concentration of 4.0×10^{-7} mol l^{-1} in a 10 ml aerated deionized water is sufficient to transform a UO_2 disc layer of 1 nm into studtite. One can also estimate the H_2O_2 concentration that is sufficient to form a 1 nm studtite layer on the leached disc surface of 0.283 cm^{-2} (6 mm diameter). For a studtite density of 3.64 g cm^{-3}, the number of studtite moles (374 g/mole) per nm on the leached surface of 0.283 cm^{-2}, is 2.75×10^{-10} moles. According to reaction (R4), this formation corresponds to a consumption of 5.5×10^{-10} H_2O_2 moles. The minimal H_2O_2 concentration is then 5.5×10^{-8} mol l^{-1} in a 10 ml volume.

In the present experiments, the fitting of the RBS spectra obtained after the different leaching times shows that only a part of the corrosion layer is transformed into

studtite. Assuming a whole transformation of the corrosion layer into studtite, one can estimate the maximal H_2O_2 concentration that is consumed during the corrosion process. For $[H_2O_2]$ addition in the range 10^{-3} or 10^{-1} mol l^{-1}, after 112 h of leaching, the H_2O_2 consumption corresponding to a whole transformation of the corrosion layers into studtite is calculated to be one to two orders of magnitude lower than the initial H_2O_2 concentration. For example, for $[H_2O_2] = 5 \times 10^{-5}$ mol l^{-1}, the corrosion layer after 112 h of leaching reaches a thickness of 112 nm according to RBS. For the consumption rate of 5.5×10^{-8} mol l^{-1} nm^{-1} determined above, the H_2O_2 concentration corresponding to the whole transformation of such a layer is of the order of 6.2×10^{-6} mol l^{-1}. This value is one order below the initial H_2O_2 concentration. These variations are too low to be detected experimentally. It is why the H_2O_2 concentrations measured initially and at the end of the leaching are the same for added H_2O_2 concentrations in the range 5×10^{-5}–10^{-1} mol l^{-1}.

It is interesting to examine which of the quantities, the H_2O_2 radiolytic production or the growth rate of the corrosion layer, controls the growth of studtite under He^{2+} beam irradiation. One can estimate roughly the time that it takes to produce the amount of H_2O_2, 5.5×10^{-8} mol l^{-1} in a 10 ml volume, necessary to form a 1 nm layer of studtite on the leached and irradiated disc surface of 0.283 cm^{-2} (6 mm diameter). According to Fig. 2, H_2O_2 is produced by irradiation at a yield of 7.4×10^{-6} mol l^{-1} J^{-1} in a 10 ml volume. To reach the H_2O_2 concentration of 5.5×10^{-8} mol l^{-1}, the beam needs to deposit a energy of 7.4×10^{-3} J. The beam considered for the calculation has the typical characteristics: E^{2+}_{He} (MeV) = 5, flux (He^{2+} cm^{-2} s^{-1}) = 3.3×10^{11}, $dE/dt\,dS$ (J s^{-1} cm^{-2}) = 2.6×10^{-1}, $dE/dt\,dS$ (J h^{-1} cm^{-2}) = 9.5×10^{2}, S (cm^{-2}) = 0.283, t (h) = 1, E (J h^{-1}) = 270). Such a beam deposits energy in the 10 ml volume through the leached surface of 0.283 cm^2 at a rate of 270 J h^{-1}. It is sufficient to irradiate the interface during 2.7×10^{-5} h or 0.099 s to produce the H_2O_2 concentration of 5.5×10^{-8} mol l^{-1} necessary to grow a 1 nm studtite layer. One can estimate the thickness of the studtite layer that can grow under irradiation during 0.099 s. For the highest value of the growth rates determined under irradiation, 112 nm h^{-1}, the studtite layer during 0.099 s reaches a thickness of only 3.1×10^{-3} nm much lower than 1 nm. This value is much lower than any of the unit-cell dimension of studtite and, even, below an atomic radius. To calculate such a value indicates that the number of moles formed after 0.099 s is so low, 8.5×10^{-13}, that the surface is only partially covered with studtite. These calculations show that it takes much less time to produce the H_2O_2 amount necessary to grow a layer of a given thickness than it takes to grow this layer. The process that limits the growth of the corrosion layer during irradiation is therefore the corrosion process itself rather than the H_2O_2 radiolytic production.

8. Implications for spent fuel disposal

The present work shows that aerated UO_2/H_2O interfaces have their properties affected under He^{2+} beam irradiation The production of hydrogen peroxide and, most likely, also of some other radiolytic species, are responsible for the changes. This information may provide insights into the evolution of spent fuel interfaces.

The formation of studtite appears as a fingerprint of the H_2O_2 radiolytic production at UO_2/H_2O interfaces under He^{2+} irradiation. It can be expected to appear at a spent fuel surface at the condition that H_2O_2 is locally produced by radiolysis in the natural water leaching spent fuel. It has indeed been observed that uranium peroxides exist in natural state. Studtite and metastudtite occur for instance at the uranium deposit of Shinkolobwe in Shaba, Zaire [29] and at the uranium deposit of Menzenschwand in the Black Forest in Germany [28]. More recently, studtite has also been observed at the surface of Chernobyl 'lava' [41,42]. Despite the building of a 'shelter' to isolate the destroyed Chernobyl reactor, the 'lava' can still be leached by water, such as rainwater, and studtite is one of the secondary phase that can be formed. The formation of studtite and metastudtite on spent fuel powders (50–250 nm particle size) has also been recently observed after 2 years of immersion in deionized water and storage at 28 °C in the dark [43–46]. As in the present experiment on UO_2, the uranium peroxide layer morphology on the spent fuel particles appears as a loose structure formed by closed bundles of thin rods. According to the authors, the thickness of the corrosion layers in some of the spent fuel particles can reach several microns.

In the assumption that spent fuel behaves as UO_2, the present experiments can be used to estimate the time that it takes for a spent fuel to produce the amount of H_2O_2 necessary to form a layer of 1 nm studtite on a 1 cm^2 surface. The spent fuel activity is assumed to produce an alpha flux that deposits energy with a density rate, $dE/dt\,dS$ (J s^{-1} cm^{-2}) = 2.6×10^{-5}. This rate corresponds to beam experiments where the flux is about four order of magnitude lower than in those typically used in the present work. One can extrapolate from Fig. 2 that this fuel produces H_2O_2 at a yield of 7.4×10^{-6} mol l^{-1} J^{-1} in a 10 ml volume. As seen in Section 7.3, the energy needed to produce the H_2 concentration used in the formation of a studtite layer of 1 nm on a 0.283 cm^2 surface is 7.4×10^{-3} J. Water needs then to stay in contact with the spent fuel surface during 2.7×10^{-1} h or 9.9×10^{2} s (16 min). To accumulate the

H_2O_2 concentration of 1.9×10^{-7} mol l^{-1} needed to form a 1 cm^2 studtite surface of a 1 nm thickness then requires only 56 mn in the same conditions.

The transformation of spent fuel into studtite can possibly result into dissemination of uranium in environment if one considers that the consequences of this transformation are similar to those observed for UO_2. The corrosion process leads to a mechanically weak layer and, in the ultimate stage of a whole transformation, produces finally a solid under a powder-form. The studtite formation on spent fuel surface may jeopardize spent fuel integrity. It seems better to avoid the formation of this phase. Once contact occurs between spent fuel and water, this situation may occur when the local chemistry at the UOX/H_2O interfaces maintains a low H_2O_2 radiolytic production that ensures sufficiently low H_2O_2 concentrations near the spent fuel surface. The presence in water of metallic impurities, as iron, that are known to decompose hydrogen peroxide can likely reduce such a production. These metallic impurities can come from the clad of spent fuel or from the stainless steel container of confinement.

It has been reported in [21] that the alteration of UO_2 in presence of Ar purge deioinzed water differs from that in a given natural neutral (pH = 7.2 [21]) Ar purge groundwater. The author relates this behaviour to that observed for the oxidation of U(IV) into U(VI) by oxygen or hydrogen peroxide. It is known that the oxidation can be activated or inhibited by the presence of specific solutes [21, references herein]. However, data are lacking to confirm such effects on the H_2O_2 radiolytic production at UO_2/H_2O interfaces for long time irradiation. It is consequently necessary to collect more information to understand the basic properties of the H_2O_2 radiolytic production at UO_2/H_2O interfaces. Work is in progress with the beam method used here to investigate the effects of aqueous solution chemistry, specially the role of metallic impurities and/or solutes that are complexing U under anoxic conditions.

9. Conclusion

This work focuses on the influence of H_2O_2 on the evolution of UO_2/H_2O interfaces as a function of leaching time. It investigates whether this time evolution is dependent on the method that introduces H_2O_2 in deionized aerated water. Two methods are used where, for similar interfaces, H_2O_2 is either added or produced at the UO_2/H_2O interfaces under He^{2+}-irradiation at high ion flux. The ratio S/V of the solid surface to the solution volume is calculated for the geometrical area and has the value 2.8 m^{-1}. The corresponding specific surface area is 3.2×10^{-6} m^2 g^{-1}. For the range of H_2O concentration that is investigated, 5×10^{-5}–10^{-1} mol l^{-1}, the conclusion is that the time evolutions of interfaces differ strikingly as a function of H_2O concentration as concern the solution. The differences are much less marked for the UO_2 solid. The same secondary phase, studtite, grows on UO_2. The H_3O^+ concentration, U release rates and, likely in the initial stages, the growth rates however differ significantly.

For aerated UO_2/H_2O interfaces where a given H_2O_2 concentration is added to deionized aerated water, the main features are the following:

(i) The U release increases during an initial step of oxidation–dissolution and then reaches saturation.
(ii) The corrosion process transforms UO_2 into a hydrated uranium peroxide, $UO_2(O_2) \cdot 4H_2O$, called studtite. The thickness of the corrosion layer measured by RBS increases linearly as a function of time, indicating a process controlled by a reaction at the interface. This reaction is either a surface reaction or a precipitation reaction induced at the hydrated UO_2 surface. The corrosion layer is not protective for the solid.
(iii) The layer growth rate, GR, increases with H_2O_2 concentration and is given by:

$$\mathrm{GR\ (nm/h)} = 295 + 92 \log([H_2O_2]),$$

$$\text{for } [H_2O_2] \geq 6.3 \times 10^{-4} \text{ mol l}^{-1}.$$

Below 1.1×10^{-3} mol l^{-1}, the corrosion rates are few manometers per hour.

For aerated UO_2/H_2O interfaces under irradiation where radiolysis in deionized aerated water produces an increasing H_2O_2 concentration as a function of leaching time, the main features are the following.

(i) UO_2 is transformed into studtite. This process is considered as a fingerprint of the H_2O_2 radiolytic production.
(ii) The total uranium release increases a function of leaching time under irradiation at a quasi-constant rate of 6.4×10^{-5} g cm^{-2} h^{-1} (2.3×10^{-7} mol cm^2 h^{-1}) for the flux 1.9×10^{11} He^{2+} cm^2 s^{-1} during at least 4 h. The energy density per surface unit is deposited with a rate of $\approx 5.6 \times 10^2$ J h^{-1} cm^{-2} in the vicinity of the surface ($\approx$30 μm) and the dose rate per volume unit is $\geqslant 5.6 \times 10^5$ Gy cm^{-3}.
(iii) The growth rate of the corrosion layer obtained in continuous or after a cycle of sequential dissolutions seems to decrease as leaching time increases. In the 10^{-3}–10^{-2} mol l^{-1} range, its value tends towards a limit $\approx$50 nm h^{-1} that is of the order of magnitude of those measured for H_2O_2 additions in this range.

Acknowledgments

The authors are grateful to ARAMIS staff for their assistance during experiments, D. Gosset (CEA-Saclay, DEN/DMN/SRMA/LMS, France) for XRD analysis and S. Ancelin (CERI-CNRS Orléans, France) for H_2O_2 analysis. This work is partially funded from the Commission of the European Communities (Contract no. FIKW-CT-2001-00192 SFS) and CEA-PRECCI project (C. Poinssot and C. Ferry, CEA-Saclay DPC/SECR).

Appendix A

The RBS analysis is performed assuming that the tetrahydrated uranium peroxide ($UO_2(O_2)$–nH_2O, $n = 4$), studtite is converted into the dehydrated uranium peroxide ($UO_2(O_2)$–nH_2O, $n = 2$) when the spectra are recorded. The spectra are then stable as a function of beam analysis. The RBS analysis gives thickness (TH_{RBS}) in units that are atom number by surface unit. To convert into length unity (TH), the density d in number of atoms by volume unit of the analysed compound should be known. The layer thickness is given by TH (length unit) $= TH_{RBS}/d$. The dehydrated uranium peroxide ($n = 2$) density is 9.16×10^{22} at cm^{-3} [16,17]. However, the composition in the altered layer varies as a function of depth from the surface ($UO_2(O_2)$–nH_2O) to the non-altered solid (UO_2). The total number of atoms in the crystallographic cell of $UO_2(O_2)$–nH_2O is given by $Z(5 + n)$, where Z is the multiplicity of the cell equal to 2 [16,17]. From the cell volume V_c of metastudtite, $V_c = 2.4 \times 10^{-22}$ cm^3 [16,17], the $UO_2(O_2)$–nH_2O density is given by $Z(5 + n)/V_c$. Thus, the density varies from $Z(5 + n)/V_c$ at the surface to 7.0×10^{22} at cm^{-3} (sintered UO_2 density) at the end of the altered layer. The RUMP fit gives the variation of composition as a function of the depth in the altered layer. So, for each value of the thickness, the density is calculated and the variation of the density as a function of the depth is obtained. Finally, the total thickness of corrosion layer is calculated.

References

[1] S. Sunder, D.W. Shoesmith, Chemistry of uranium dioxide fuel dissolution in relation to the disposal of used nuclear fuel, Atomic Energy of Canada Limited, Report AECL-10395, 1991.
[2] D.W. Shoesmith, S. Sunder, An electrochemistry-based model for the dissolution of uranium dioxide, Atomic Energy of Canada Limited, AECL-10488, 1991.
[3] D.W. Shoesmith, S. Sunder, J. Nucl. Mater. 190 (1992) 20.
[4] L.H. Johnsson, D.W. Shoesmith, in: W. Lutze, R.C. Ewing (Eds.), Radioactive Waste Forms for the Future, North-Holland, Amsterdam, 1988, p. 635.
[5] D.W. Shoesmith, L.H. Johnsson, Models for used nuclear fuel corrosion under waste disposal conditions, Ontario Hydro Report No. 06819-REP-01200-0012 R00, 1997.
[6] H. Christensen, S. Sunder, Current state of knowledge in radiolysis effects on spent fuel corrosion, Studvisk Material AB, Nykoping, Sweden, Report # STUDSVIK/M-98/71, 1998.
[7] W.J. Gray, Pacific Northwest Laboratory, PNL/SRP-6689, 1988.
[8] H. Christensen, S. Sunder, D.W. Shoesmith, J. Alloys Compd. 213/214 (1994) 93.
[9] A.O. Allen, The Radiation Chemistry of Water and Aqueous Solutions, D. Van Nostrand Co., Princeton, 1961.
[10] J.W.T. Spinks, R.J. Woods, An Introduction to Radiation Chemistry, 3rd Ed., Wiley-Interscience, New York, 1990.
[11] C. Corbel, J.-F. Lucchini, G. Sattonnay, M.-F. Barthe, F. Huet, P. Dehaudt, C. Ardois, B. Hickel, J.L. Paul, Mat. Res. Soc. Symp. Proc. 608 (2000).
[12] G. Sattonnay, C. Ardois, C. Corbel, J.F. Lucchini, M.-F. Barthe, F. Garrido, D. Gosset, J. Nucl. Mater. 288 (2001) 11.
[13] C. Corbel, G. Sattonnay, J.-F. Lucchini, C. Ardois, M.-F. Barthe, F. Huet, P. Dehaudt, C. Ardois, B. Hickel, C. Jegou, Nucl. Instrum. and Meth. B 179 (2001) 225.
[14] J.B. Hiskey, Inst. Min. Metall. Trans. Sec. C 89 (1980) C145.
[15] L.E. Eary, L.M. Cathles, Metall. Trans. B 14B (1983) 325.
[16] H. Christensen, Mater. Res. Soc. Symp. Proc. 212 (1991) 213.
[17] P. Diaz-Arocas, J. Quinones, C. Maffiotte, J. Serrano, J. Garcia, J.R. Almazan, J. Esteban, Mater. Res. Soc. Symp. Proc. 353 (1995) 641.
[18] J. Giminez, E. Baraj, M.E. Torrero, I. Casas, J. de Pablo, J. Nucl. Mater. 238 (1996) 64.
[19] J. de Pablo, I. Casas, J. Giminez, V. Martti, M.E. Torrero, J. Nucl. Mater. 232 (1996) 138.
[20] J. de Pablo, I. Casas, F. Clarens, F. El Aammrani, M. Rovira, Mat. Res. Soc. Symp. Proc. 663 (2001) 409.
[21] M. Amme, Radiochim. Acta 90 (2002) 399.
[22] M. Amme, B. Renker, B. Schmid, M.P. Feth, H. Bertagnoli, W. Döbelin, JNM 306 (2002) 202.
[23] J.F. Ziegler, J.P. Biersack, U. Littmark, The Stopping and Range of Ions in Solids, Pergamon, New York, 1985.
[24] A.O. Allen, J. Hochanadel, J.A. Ghormley, T.W. Davis, J. Phys. Chem. 56 (1952) 575.
[25] J. Hochanadel, J. Phys. Chem. 56 (1952) 587.
[26] L.R. Doolittle, Nucl. Instrum. and Meth. B 9 (1985) 344.
[27] P.C. Debets, J. Inorg. Nucl. Chem. 25 (1963) 727.
[28] K. Walenta, Am. Mineral. 59 (1974) 166.
[29] M. Deliens, P. Piret, Am. Mineral. 68 (1983) 456.
[30] G.W. Watt, S.L. Achorn, J.L. Marley, J. Am. Chem. Soc. 72 (1950) 3341.
[31] G. Gordon, H. Taube, J. Inorg. Nucl. Chem. 16 (1961) 268.
[32] C. Rocchiccioli, C. R. Acad. Sci., Ser. A B 263B (1966) 1061.
[33] P. Burns, K. Hughes, Am. Miner. Dept. 88 (2003) 1165.

[34] P. Clarens, J. de Pablo, J. Diez_Perez, I. Casas, J. Gimenez, M. Roviera, Environ. Sci. Technol. 38 (2004) 6656.
[35] I. Casas, J. Gimenez, V. Marti, M.E. Torrero, J. de Pablo, Radiochim. Acta 66/67 (1994) 23.
[36] I. Grenthe, J. Fuger, R.J.M. Konings, R.J. Lemire, A.B. Muller, C. Nguyen-Trung, H. Wanner, Chemical thermodynamics of uranium, Chemical thermodynamics 1, OECD, 1992.
[37] L.J. Brady, C.D. Susano, C.E. Larson, Chemical and Physical Properties of Uranium Peroxide, United States Atomic Energy Commission, Oak Ridge, AECD-2369, 1948.
[38] K.A. Hughes Kubatko, K.B. Helean, A. Navrotsky, P.C. Burns, Science 302 (2003) 1191.
[39] P. Marcus (Ed.), Corrosion Mechanism in Theory and Practice, 2nd Ed., Dekker, 2002.
[40] R.A. Berner, in: A.C. Lasaga, R.J. Kirkpatrick (Eds.), Reviews in Mineralogy, vol. 8, Mineralogical Society of America, Washington, DC, 1981, p. 111.
[41] E.B. Anderson, B.E. Burakov, E.M. Pazukhin, Radiokhimiya 34 (1992) 135.
[42] B.E. Burakov, E.E. Strykanova, E.B. Anderson, Mater. Res. Soc. Symp. Proc. 465 (1997) 1309.
[43] B. Mc Namara, E. Buck, B. Hanson, Mat. Res. Soc. Proc. 757 (2003).
[44] B. McNamara, B. Hanson, E. Buck, C. Soderquist, Mat. Res. Soc. Proc. 824 (2004) 139.
[45] B. McNamara, B.D. Hanson, E. Buck, C. Soderquist, Radiochim. Acta 93 (2005) 169.
[46] B. Hanson, B. McNamara, E. Buck, J. Friese, E. Jenson, K. Krupka, B.W. Arey, Radiochim. Acta 93 (2005) 159.